

## Supporting Information

### **New palladium(II) and platinum(II) complexes with ONS donor azo-thioether pincer ligand: Synthesis, characterization, protein binding study and in vitro cytotoxicity**

**Akash Das,<sup>a</sup> Moumita Saha,<sup>b</sup> Subrata Mandal,<sup>a</sup> Sanjib Das,<sup>b</sup> Krishna Das Saha<sup>\*b</sup> and Tapan K. Mondal<sup>\*a</sup>**

<sup>a</sup>Department of Chemistry, Jadavpur University, Kolkata- 700032, India. E-mail: [tapank.mondal@jadavpuruniversity.in](mailto:tapank.mondal@jadavpuruniversity.in)

<sup>b</sup>Cancer Biology & Inflammatory Disorder Division, CSIR-Indian Institute of Chemical Biology, Kolkata – 700 032, India

### CONTENTS

Fig. S1: <sup>1</sup>H-NMR spectrum of [Pd(L)Cl] (**1**) in CDCl<sub>3</sub>

Fig. S2: <sup>1</sup>H-NMR spectrum of [Pt(L)Cl] (**2**) in CDCl<sub>3</sub>

Fig. S3: HRMS of Pd(II) complex

Fig. S4: HRMS of Pt(II) complex

Fig. S5: IR spectrum of free HL

Fig. S6: IR spectrum of complex **1**

Fig. S7: IR spectrum of complex **2**

Table S1: Crystallographic data and refinement parameters of complexes **1** and **2**

Table S2: Selected X-ray and calculated bond distances and angles of complexes **1** and **2**

Table S3: Energy and composition of some selected molecular orbitals of **Pd(II)** complex

Table S4: Energy and composition of some selected molecular orbitals of **Pt(II)** complex

Table S5: Vertical electronic transition calculated by TDDFT/CPCM method of complexes **1** and **2**

Fig. S8: 1-D supramolecular structure of **2** formed by Cl...H and O...H bonding interactions.

Fig. S9: Contour plots of some selected molecular orbital of **Pd(II)** complex (**1**)

Fig. S10: Contour plots of some selected molecular orbital of **Pt(II)** complex (**2**)

Fig. S11: Spin density plots of (A) **1**<sup>+</sup> and (B) **2**<sup>+</sup>

Fig. S12: Spin density plots of (A) **1**<sup>-</sup> and (B) **2**<sup>-</sup>

Fig. S13: Plot of log [(F<sub>o</sub>-F)/F] versus log [complex] of **Pd(II)** complex (A) and **Pt(II)** complex (B)

Fig. S14: (A) Viability of A549, HepG2 and HCT116 cells were assessed by treating different dose of HL and (B) the effects of [Pd(L)Cl] (**1**) and [Pt(L)Cl] (**2**) in peripheral blood mononuclear cells (PBMCs)

Fig. S15: Viability of A549, HepG2 and HCT116 cells towards doxorubicin (Dox)

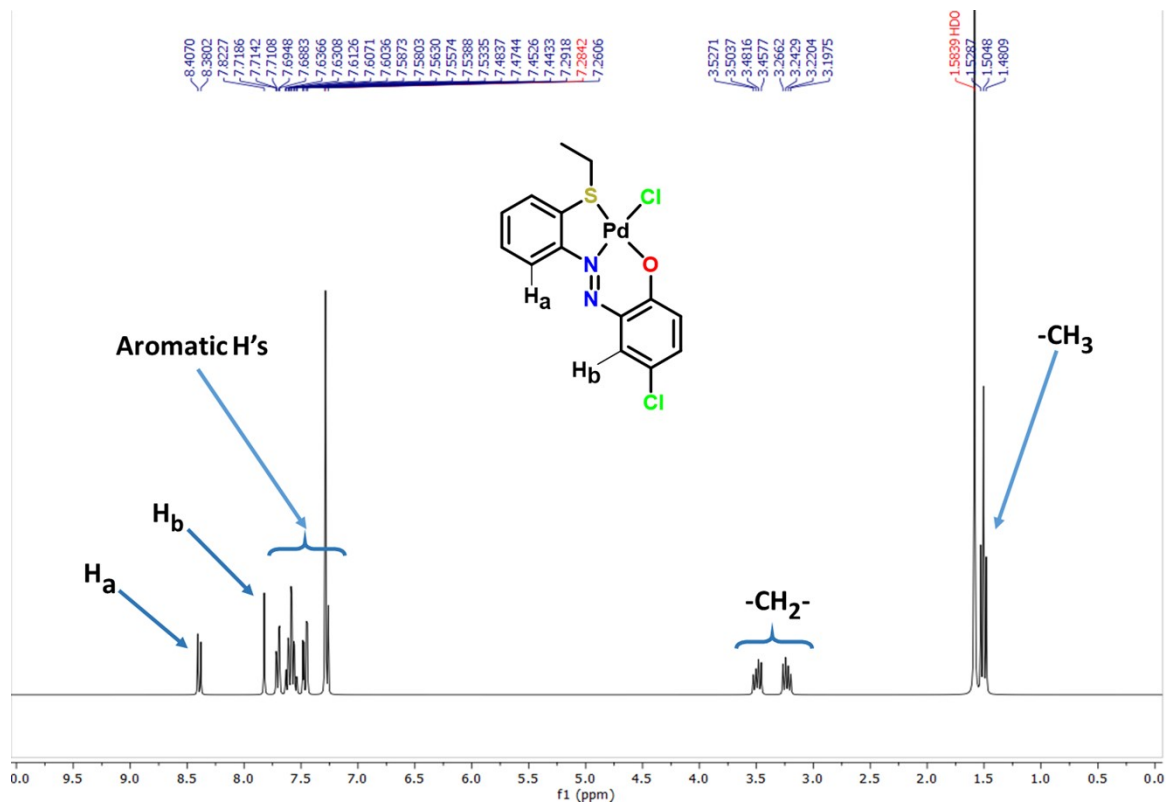


Figure S1: <sup>1</sup>H-NMR spectrum of [Pd(L)Cl] (1) in CDCl<sub>3</sub>

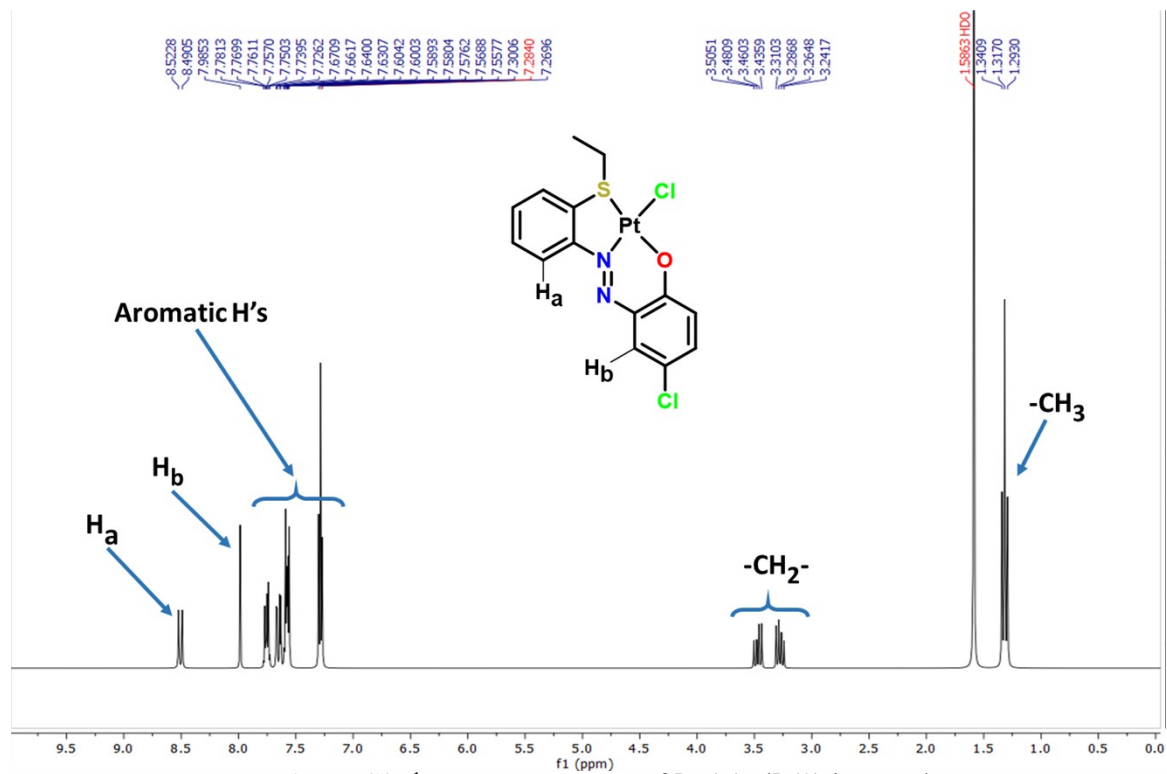
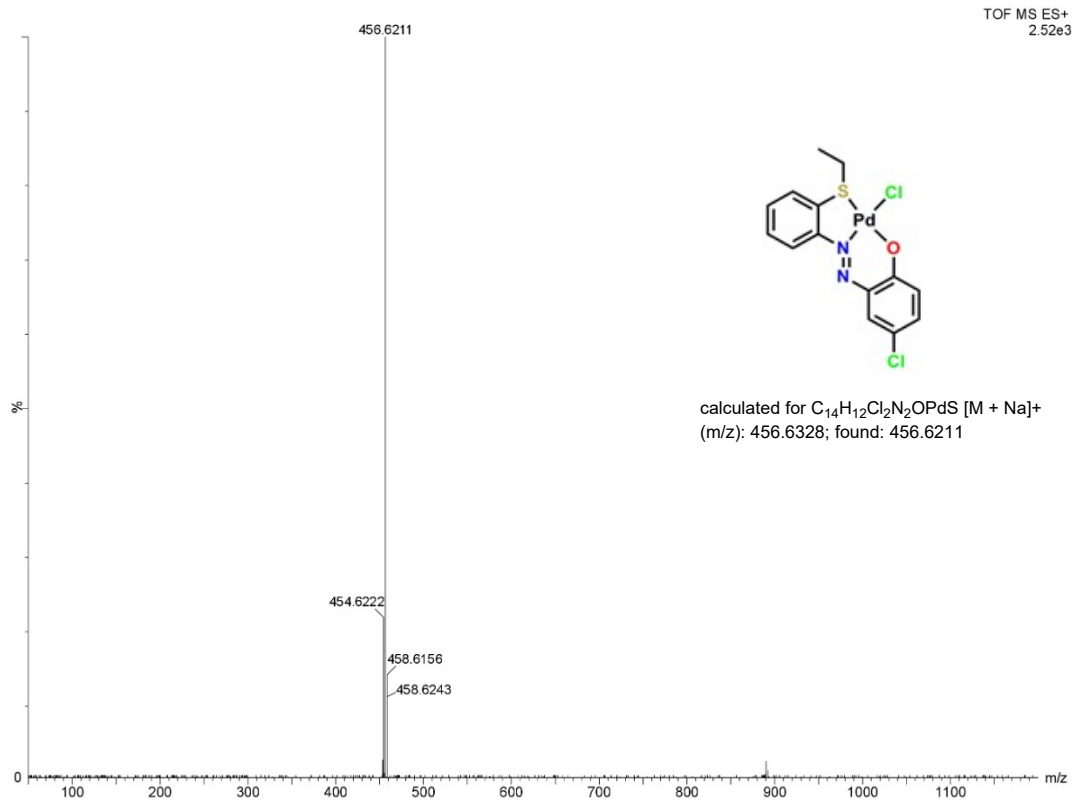
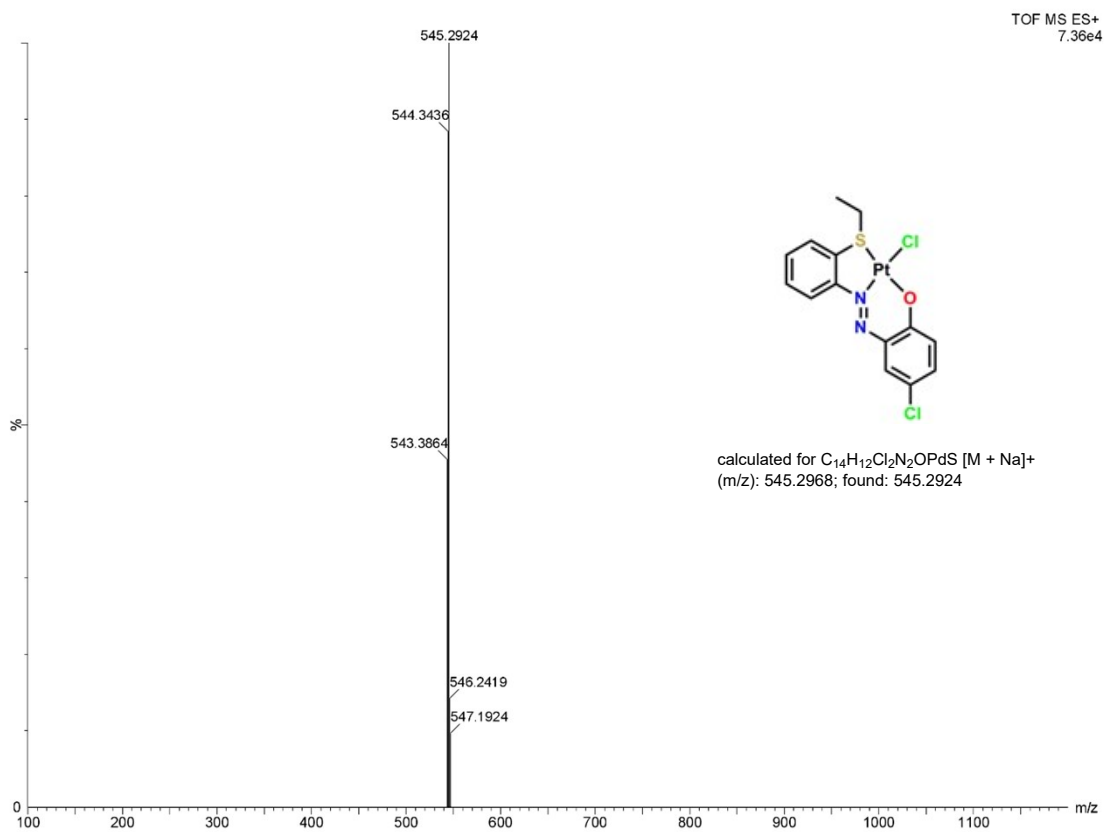


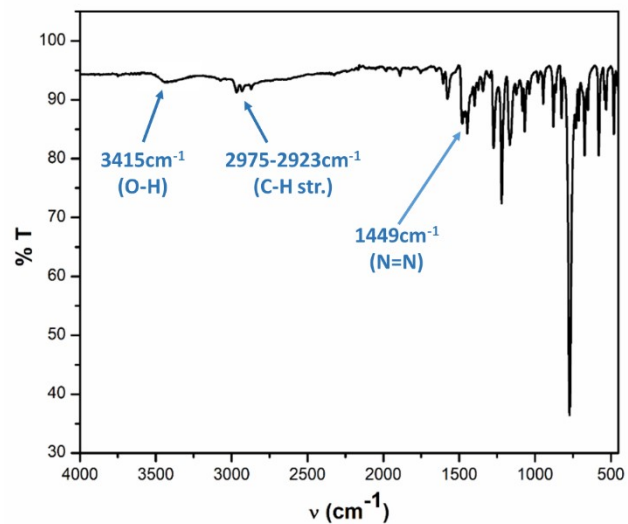
Figure S2: <sup>1</sup>H-NMR spectrum of [Pt(L)Cl] (2) in CDCl<sub>3</sub>



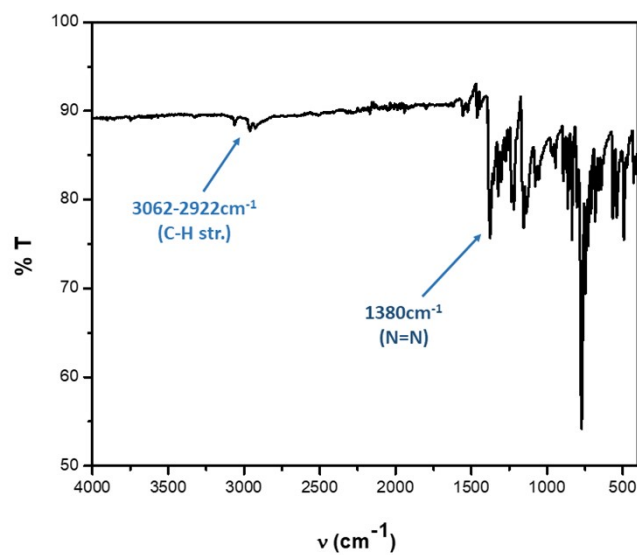
**Figure S3:** HRMS spectrum of [Pd(L)Cl] (1)



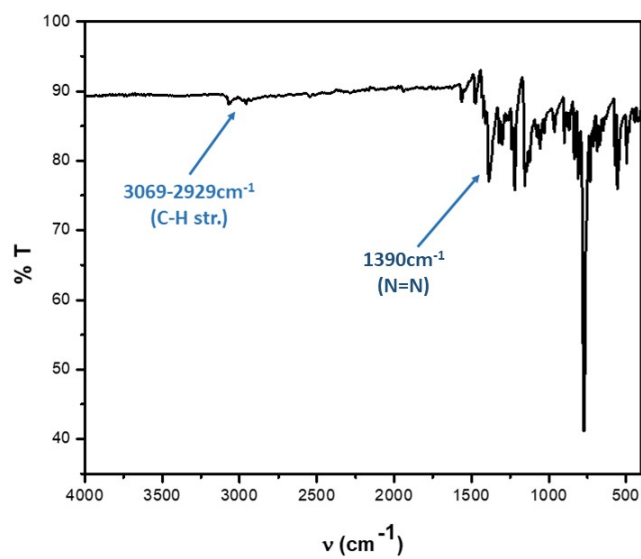
**Figure S4:** HRMS spectrum of [Pt(L)Cl] (2)



**Figure S5:** IR spectrum of free HL



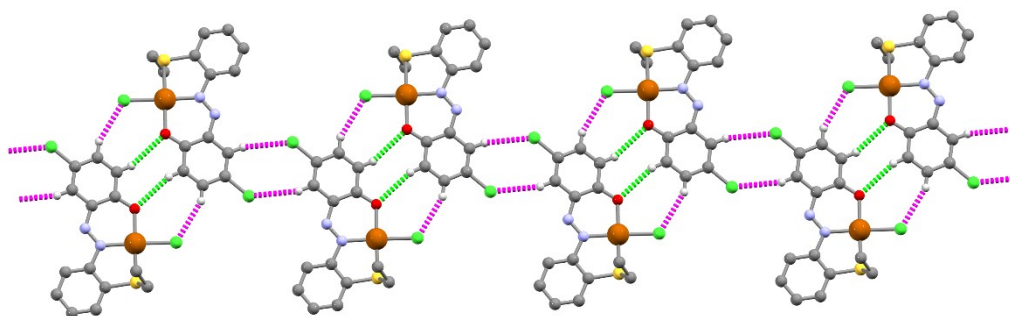
**Figure S6:** IR spectrum of complex 1



**Figure S7:** IR spectrum of complex 2

**Table S1:** Crystallographic data and refinement parameters of **1** and **2**

Formula	C <sub>14</sub> H <sub>12</sub> Cl <sub>2</sub> N <sub>2</sub> OPdS	C <sub>28</sub> H <sub>24</sub> Cl <sub>4</sub> N <sub>4</sub> O <sub>2</sub> Pt <sub>2</sub> S <sub>2</sub>
Formula Weight	433.62	1044.61
Crystal System	<i>triclinic</i>	<i>triclinic</i>
Space group	<i>P</i> 1	<i>P</i> 1
a, b, c [Å]	7.4987(6), 9.4330(7), 11.6092(9)	10.1219(11), 12.2233(13), 13.6071(15)
α	101.126(2)	109.453(3)
β	103.873(2)	95.228(3)
γ	98.613(2)	96.489(3)
V [Å <sup>3</sup> ]	765.50(10)	1562.3(3)
Z	2	2
D(calc) [g/cm <sup>3</sup> ]	1.881	2.221
Mu(MoKa) [ /mm]	1.695	9.455
F(000)	428	984
Temperature (K)	293(2)	293(2)
Radiation [Å]	0.71073	0.71073
θ(Min-Max) [°]	2.554- 27.217	1.943- 27.542
Dataset (h; k; l)	-9 to 9, -12 to 12, -14 to 14	-13 to 13, -15 to 15, -17 to 17
R, wR <sub>2</sub>	0.0278, 0.0748	0.0249, 0.0595
Goodness of fit(S)	1.094	1.023
CCDC No.	2178572	2178573

**Figure S8:** 1-D supramolecular structure of **2** formed by Cl...H and O...H bonding interactions.

**Table S2:** Selected X-ray and calculated bond distances and angles of complexes **1** and **2**

Bonds(Å)	[Pd(L)Cl] ( <b>1</b> )		[Pt(L)Cl] ( <b>2</b> )	
	X-ray	Calc.	X-ray	Calc.
Pd1–N1	1.979(2)	2.017	1.966(3)	2.00813
Pd1–O1	1.9960(18)	2.018	2.000(3)	2.02230
Pd1–S1	2.2401(6)	2.301	2.2316(12)	2.29275
Pd1–Cl1	2.3106(7)	2.341	2.3126(11)	2.35894
Cl2–C4	1.738(3)	1.756	1.745(5)	1.75638
S1–C12	1.771(3)	1.797	1.774(5)	1.79677
S1–C13	1.821(3)	1.857	1.824(5)	1.85930
O1–C1	1.291(3)	1.285	1.306(5)	1.29344
N1–N2	1.270(3)	1.277	1.283(5)	1.27865
N1–C7	1.448(3)	1.431	1.444(5)	1.43421
Angles (°)				
N1–Pd1–O1	93.06(8)	92.058	93.37(13)	92.52811
N1–Pd1–S1	87.71(6)	86.946	87.64(10)	87.05536
O1–Pd1–S1	178.54(6)	177.927	177.71(9)	178.30795
N1–Pd1–Cl1	175.99(6)	176.199	176.21(10)	177.60868
O1–Pd1–Cl1	90.84(5)	91.046	89.14(9)	89.26697
S1–Pd1–Cl1	88.41(3)	90.019	89.96(4)	91.19538
C12–S1–C13	102.64(12)	103.691	103.1(2)	103.55565
C12–S1–Pd1	98.10(9)	97.325	98.38(15)	97.60226
C13–S1–Pd1	106.66(9)	107.014	108.44(16)	107.83721
N2–N1–Pd1	127.66(16)	127.164	128.1(3)	127.33641

**Table S3:** Energy and % of composition of some selected molecular orbitals of complex **1**

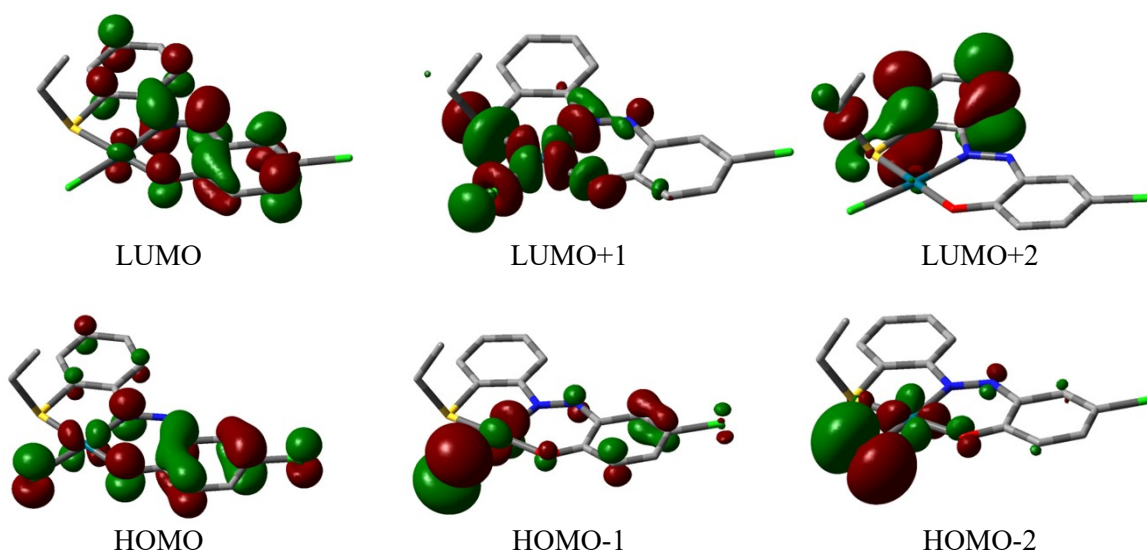
MO	Energy (eV)	% Composition		
		Pd	L	Cl
LUMO+5	-0.04	83	17	0
LUMO+4	-0.21	01	99	0
LUMO+3	-0.66	01	99	0
LUMO+2	-1.44	03	97	03
LUMO+1	-2.28	47	39	14
LUMO	-3.03	03	97	03
HOMO	-5.88	10	80	10
HOMO-1	-6.55	17	20	63
HOMO-2	-6.57	16	10	74
HOMO-3	-7.02	75	14	11
HOMO-4	-7.11	05	85	09
HOMO-5	-7.32	12	66	22
HOMO-6	-7.54	31	64	05
HOMO-7	-7.86	34	65	01
HOMO-8	-8.18	20	73	07
HOMO-9	-8.37	19	64	17
HOMO-10	-8.47	41	49	09

**Table S4:** Energy and % of composition of some selected molecular orbitals of complex **2**

MO	Energy (eV)	% Composition		
		Pt	L	Cl
LUMO+5	-0.04	51	48	01
LUMO+4	-0.23	01	99	0
LUMO+3	-0.68	01	99	0
LUMO+2	-1.46	06	93	01
LUMO+1	-1.50	44	45	11
LUMO	-3.01	05	95	0
HOMO	-5.81	17	70	13
HOMO-1	-6.49	22	35	42
HOMO-2	-6.55	21	07	72
HOMO-3	-6.96	90	07	03
HOMO-4	-7.12	13	76	11
HOMO-5	-7.36	25	65	09
HOMO-6	-7.48	18	57	25
HOMO-7	-7.82	17	80	02
HOMO-8	-8.16	20	69	11
HOMO-9	-8.42	28	53	19
HOMO-10	-8.48	26	61	13

**Table S5:** Vertical electronic transition calculated by TDDFT/CPCM method of complexes **1** and **2**

Compd.	$\lambda$ (nm)	E (eV)	Osc. Strength (f)	Key excitations	Character	$\lambda_{\text{expt.}}$ (nm) ( $\epsilon$ , $M^{-1}cm^{-1}$ )
<b>1</b>	535.9	2.3134	0.1505	(84%)HOMO→LUMO	ILCT	550 (12302)
	507.5	2.4429	0.0180	(82%)HOMO→LUMO+1	LMCT/ ILCT	520 (sh.)
	368.5	3.3643	0.0861	(67%)HOMO-1→LUMO	XLCT/MLCT	372 (sh.)
	348.4	3.5586	0.2497	(67%)HOMO-4→LUMO	ILCT	338 (18162)
	340.8	3.6383	0.0893	(66%)HOMO-5→LUMO	ILCT	
<b>2</b>	544.1	2.2786	0.1444	(96%)HOMO→LUMO	ILCT/MLCT	557 (15077)
	382.1	3.2452	0.0589	(72%)HOMO-1→LUMO	XLCT/MLCT	374 (sh.)
	353.0	3.5123	0.2993	(78%)HOMO-4→LUMO	ILCT	343 (23742)
	336.1	3.6893	0.1345	(75%)HOMO-5→LUMO	ILCT	

**Figure S9:** Contour plots of some selected molecular orbital of Pd(II) complex (**1**)



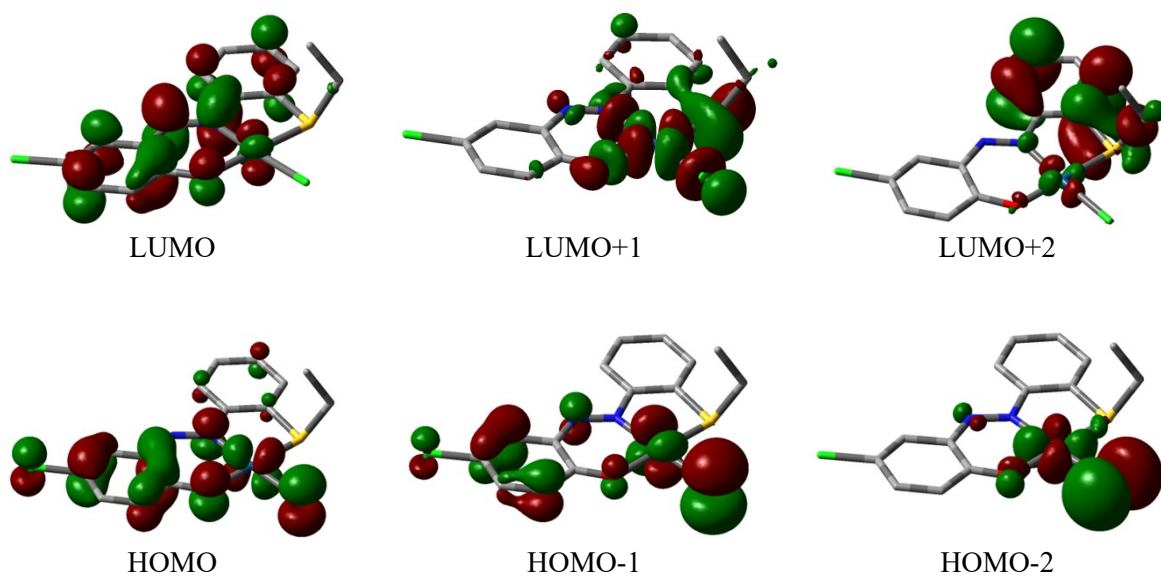


**Figure S10:** Contour plots of some selected molecular orbital of **Pt(II)** complex (**2**)

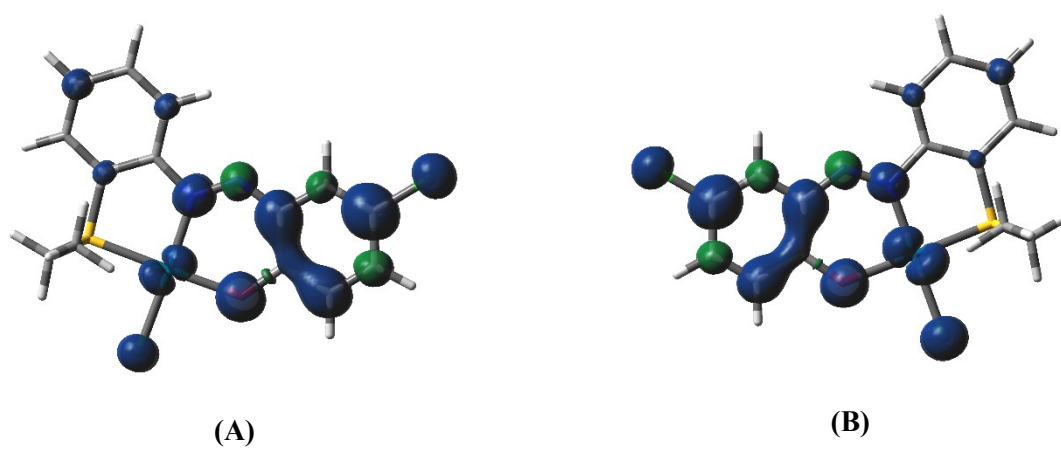


**Figure S11:** Spin density plots of (A)  $1^+$  and (B)  $2^+$

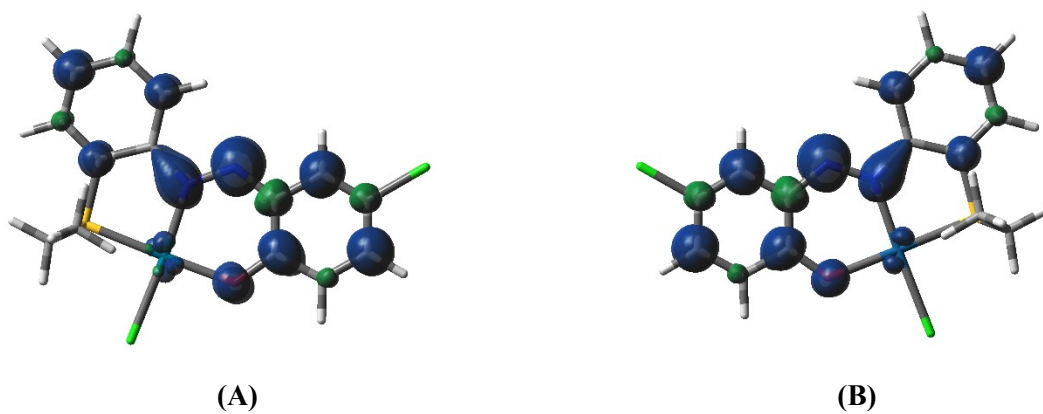


Figure S12: Spin density plots of (A) 1<sup>-</sup> and (B) 2<sup>-</sup>

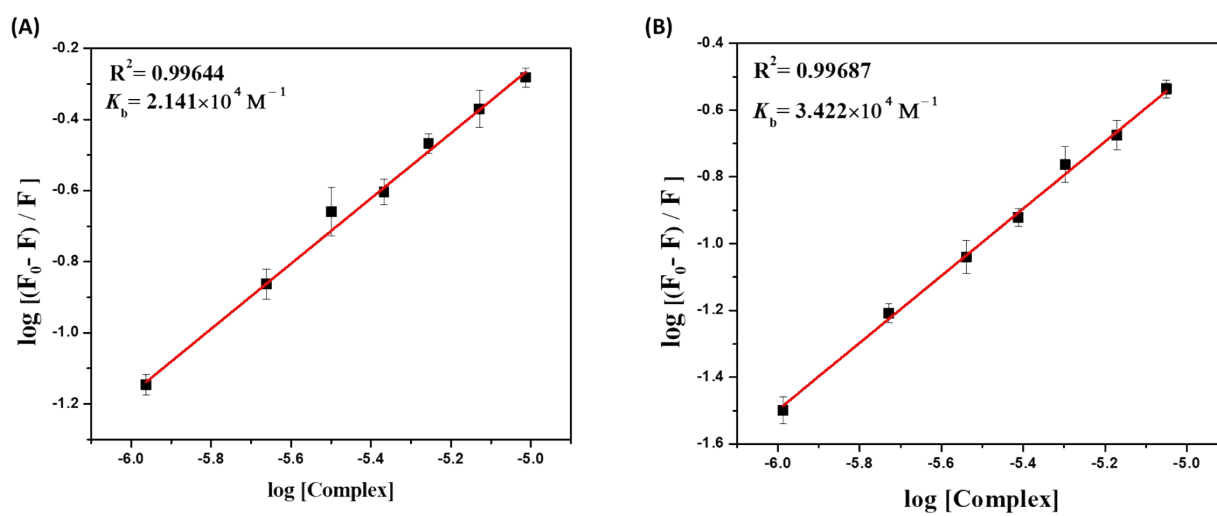
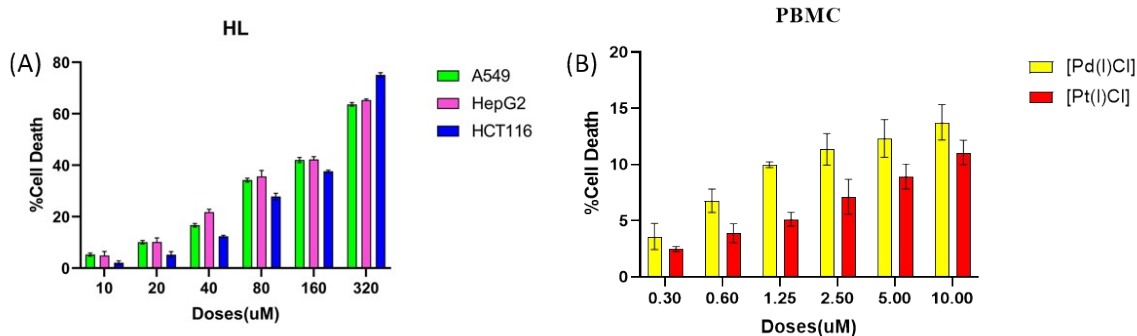
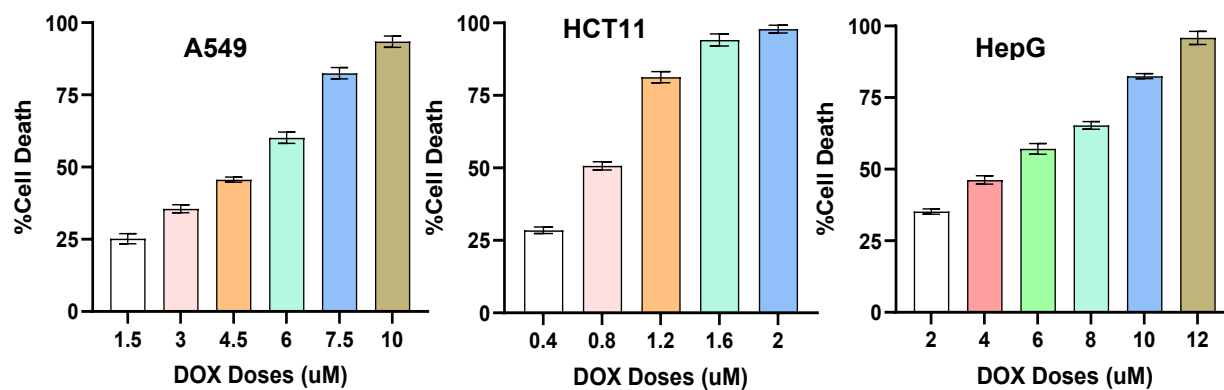


Figure S13: Plot of  $\log [(F_0 - F) / F]$  versus  $\log [\text{complex}]$  of Pd(II) complex (A) and Pt(II) complex (B)



**Figure S14:** (A) Viability of A549, HepG2 and HCT116 cells were assessed by treating different doses of HL, (B) The effects of [Pd(L)Cl] (1) and [Pt(L)Cl] (2) in peripheral blood mononuclear cells (PBMCs).



**Figure S15:** Viability of A549, HepG2 and HCT116 cells were assessed by treating different doses of Doxorubicin (Dox)